




# Discussion on spectral, electrical and third-order nonlinear optical susceptibility of semi-organic tris(cyclohexylammonium) tris(o-chlorobenzoate) dihydrate single crystal

M. Loganayaki<sup>1,\*</sup> , K. Senthil<sup>2</sup>, S. Nandhini<sup>3</sup>, A. Senthil<sup>2</sup>, P. Murugakoothan<sup>3</sup>, and G. Vinitha<sup>4</sup>

<sup>1</sup>PG and Research Department of Physics, Queen Mary's College, Chennai 600 004, India

<sup>2</sup>Department of Physics, SRM Institute of Science and Technology, Ramapuram Campus, Chennai 600 089, India

<sup>3</sup>MRDL, PG and Research Department of Physics, Pachaiyappa's College, Chennai 600 004, India

<sup>4</sup>Division of Physics, School of Advanced Science, VIT University, Chennai 600 127, India

**Received:** 16 September 2020

**Accepted:** 20 October 2020

**Published online:**  
24 November 2020

© Springer Science+Business Media, LLC, part of Springer Nature 2020

## ABSTRACT

A semi-organic single crystal named tris(cyclohexylammonium) tris(o-chlorobenzoate) dihydrate (TCTCDH) had been successfully grown applying slow evaporation procedure. The developed crystal was involved for various characterization techniques. The structural property of the sample had been analyzed employing powder XRD study. The FT-IR spectral study was applied to confirm the existence of functional groups in the title compound. The optical property of the grown material has been explored using UV-visible NIR spectral study. The dielectric constant and dielectric loss were calculated to analyze the electrical property of the titular crystal. The third-order nonlinear susceptibility of the grown material was studied employing Z-scan technique using semiconductor laser at 532 nm. The thermal behavior of TCTCDH compound was ascertained using thermo-gravimetric analysis (TGA) and differential scanning calorimetry (DSC) analysis. The Vicker's hardness study was employed to determine the mechanical stability of TCTCDH compound.

## 1 Introduction

Crystals with nonlinear optical properties play a major role in photonic technology for numerous promising utilizations such as optical signal processing, frequency mixing, ultrafast optical switches,

telecommunication systems and optical sensors [1]. Organic nonlinear optical materials are needed for optoelectronic applications owing to their high nonlinear activity, structurally more diverse and superior flexibilities but such materials suffer from disadvantages like poor mechanical and thermal strength [2].

Address correspondence to E-mail: ganeshloghi@gmail.com

The inorganic materials afford advantages such as high mechanical strength and good physiochemical stability. However, inorganic NLO crystals possess disadvantages, like modest optical nonlinearity and structural inflexibility [3]. In order to combine the advantages of organic and inorganic materials, a new class of materials has been proposed namely, the semi organics [4–7].

A new strategy of synthesizing organic–inorganic hybrid compounds has recently been very successful. Consequently, current research work focus on semi-organic materials because of their effective nonlinear coefficient, large resistance to laser-induced damage, wide phase match angle and high mechanical strength. Delocalized electrons of the organic ligands help to increase nonlinear and electro-optical activities in the semi-organic materials.

Supramolecular networks are of great interest since their intermolecular noncovalent interactions are used to plan and produce functional materials [8–10]. Carboxylic acids are generally used as hydrogen-bonding building blocks for generating stable supramolecular structures. The cyclohexylamine, a powerful base can simply react with each acid to produce salts. Cyclohexylammonium cations act as polydentate hydrogen bond donors, binding neighboring atoms by means of N-H-O bonding developing supramolecular networks and hence, a large number of cyclohexylamine derivatives have been studied for NLO applications [11–16]. In the present work, cyclohexylamine reacts with *o*-chlorobenzoic acid to form a novel NLO crystal named tris(cyclohexylammonium) tris(*o*-chlorobenzoate) dihydrate (TCTCDH) [8]. In this research work, spectral, optical, mechanical and third-order nonlinear properties of the grown material is discussed in detail. The work is also extended to report the photonic emission of the TCTCDH crystal based on photoluminescence study which is still under investigation.

## 2 Synthesis and crystal growth

Tris(cyclohexylammonium) tris(*o*-chlorobenzoate) dihydrate (TCTCDH) material was synthesized from dissolving high purity grade cyclohexylamine and *o*-chlorobenzoic acid in methanol solution in an equimolar ratio. Acidic solution provides a proton to cyclohexylamine which is base and the salt of the

relevant acid is formed. The reaction scheme of the title compound is shown in Fig. 1. After 7 h of continuous stirring the prepared solution to reach homogenous temperature and concentration all over it at room temperature, it was filtered using Whatmann filter paper to get rid of non-miscible impurities and kept for the process of formation of crystal through slow evaporation technique. By repeating recrystallization process many times, the purity of the grown material was improved. Figure 2 shows transparent and colorless crystal of dimension  $8 \times 3 \times 2 \text{ mm}^3$  yielded in a period of 18 days.

## 3 Results and discussion

### 3.1 XRD analysis

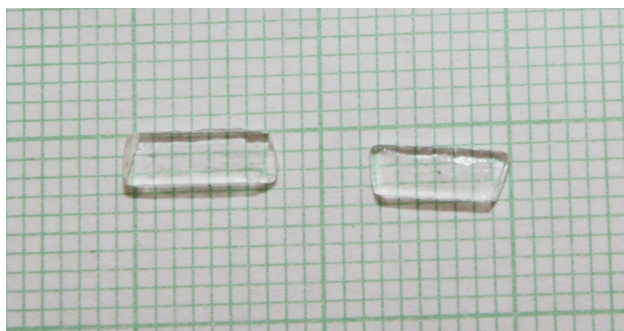
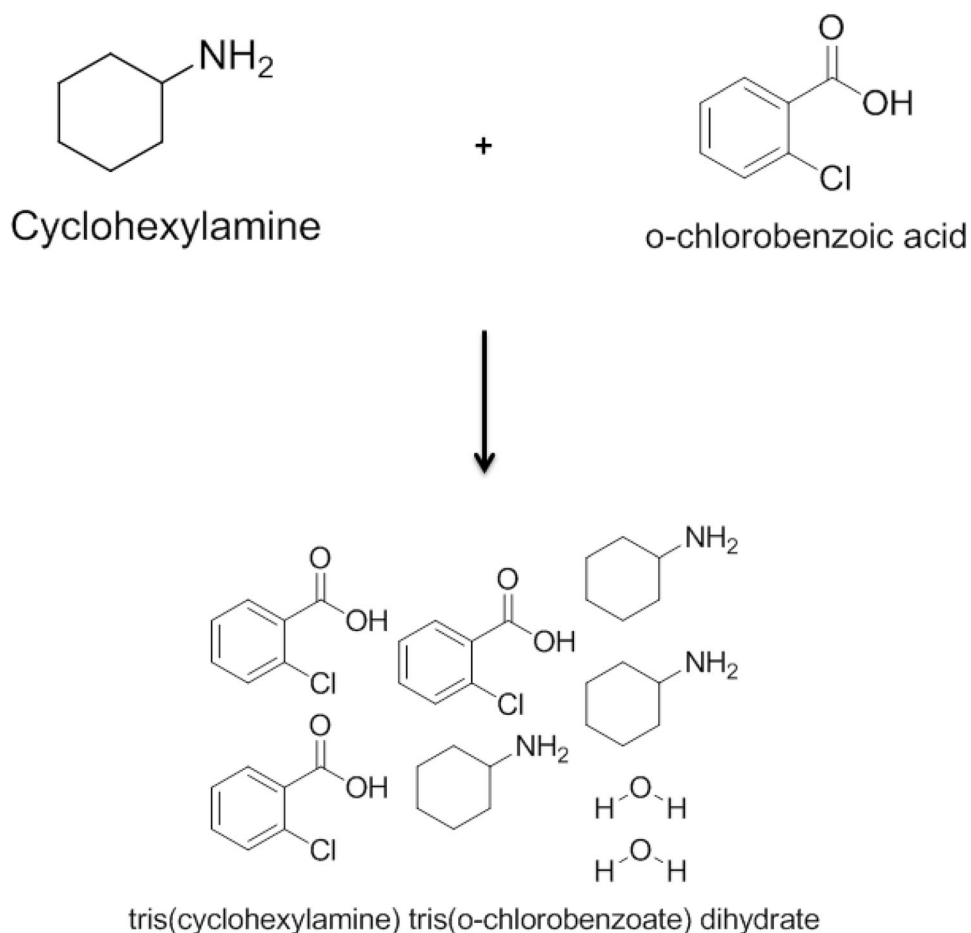
The title compound was exposed to single crystal XRD study. Its crystal system is identified as triclinic with space group P-1. To demonstrate crystallinity and to index the various planes available in the grown material, the powder XRD study was accomplished employing ISO EBYEFLEX2000 diffractometer using  $\text{CuK}\alpha$  radiation ( $\lambda = 1.5418 \text{ \AA}$ ). The well ground powder sample was evaluated in steps over  $2\theta$  range from  $10^\circ$  to  $80^\circ$  at a scan speed of  $0.02^\circ/\text{min}$  and is shown in Fig. 3. The XRD pattern shows that the majority of Bragg's peaks in the material are well-defined and sharp indicating that it is highly crystalline in nature. The obtained cell parameters are,  $a = 10.151 \text{ \AA}$ ,  $b = 13.160 \text{ \AA}$  and  $c = 17.172 \text{ \AA}$  with  $\alpha = 72.159^\circ$ ,  $\beta = 79.546^\circ$  and  $\gamma = 78.285^\circ$ . The obtained values are consistent with the reported values which are tabulated in Table 1.

### 3.2 FT-IR analysis

FT-IR is a quantitative measurement technique used for revealing the existence of the functional groups in the crystals. It is the best way to analyze purity and the structure of a material. Figure 4 shows the FT-IR spectrum of TCTCDH recorded from  $400 \text{ cm}^{-1}$  to  $4000 \text{ cm}^{-1}$  applying KBr pressed pellet technique.

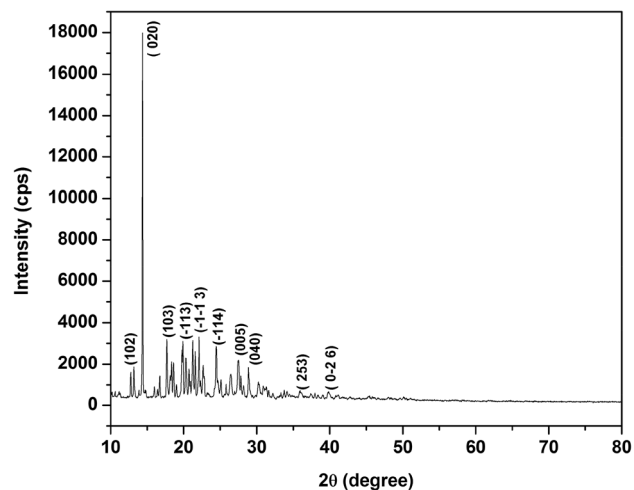
The presence of electron-donor-acceptor complex between cyclohexylamine and *o*-chlorobenzoic acid is evident by the occurrence of the characteristic spectral bands of the donor and acceptor entities in the crystal. The peak at  $3444 \text{ cm}^{-1}$  is attributed to the stretching vibration of  $\text{NH}_3^+$  bond of

**Fig. 1** Reaction scheme of TCTCDH crystal



**Fig. 2** As grown single crystal of TCTCDH

cyclohexylammonium cation. The vibrational modes at 2923 and 2854  $\text{cm}^{-1}$  indicate C–H stretching [17]. The wavenumber at 2146  $\text{cm}^{-1}$  was assigned to C–C symmetrical stretching. The less intense peak at 1612  $\text{cm}^{-1}$  confirms the presence of  $\text{H}_2\text{O}$  molecule [18] and C–O stretching at 1369  $\text{cm}^{-1}$  reveals the existence of carboxylate anion in the crystal. The absorption at 757  $\text{cm}^{-1}$  was assigned to  $\text{COO}^-$  scissoring.  $\text{COOH}$  rocking was ascribed to the peak

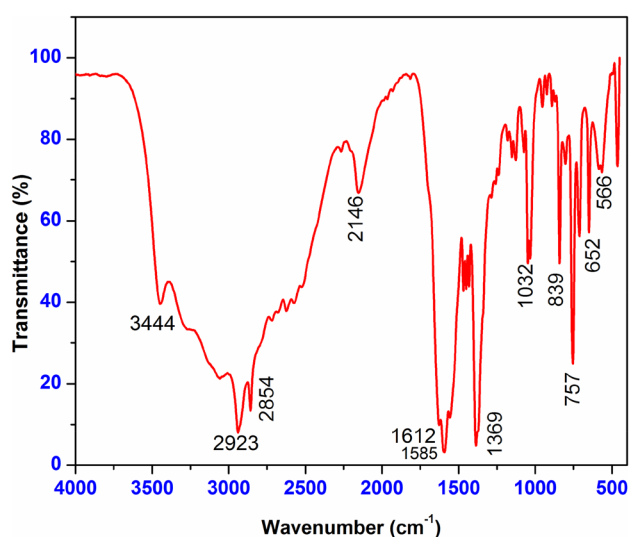


**Fig. 3** XRD pattern of TCTCDH crystal

observed at 652  $\text{cm}^{-1}$ . The absorptions at 1585  $\text{cm}^{-1}$ , 1032  $\text{cm}^{-1}$  and 839  $\text{cm}^{-1}$  indicate  $\text{NH}_3^+$  symmetrical bending [19], C–N symmetric stretching and C–Cl stretching, respectively. The observed vibrational

**Table 1** XRD data of TCTCDH crystal

Parameters of cell	Obtained value		Reported value [8]
	SXRD	PXRD	
Crystal system	Triclinic	Triclinic	Triclinic
a (Å)	10.151	10.151	10.151
b (Å)	13.160	13.160	13.160
c (Å)	17.172	17.172	17.172
$\alpha$ (°)	72.159	72.159	72.159
$\beta$ (°)	79.54	79.54	79.54
$\gamma$ (°)	78.285	78.285	78.285

**Fig. 4** FT-IR spectrum of TCTCDH

frequencies and their peak assignments are listed in Table 2.

### 3.3 Evaluation of optical parameters

Transmission spectrum is one of the essential aspects to figure out the potential of a NLO material. The UV-visible-NIR spectrum of finely polished TCTCDH crystal with 1 mm thickness was recorded between 200 and 1100 nm using VARIN CARY 5E UV-visible-NIR spectrophotometer. The resultant transmittance spectrum of TCTCDH is given in Fig. 5. The grown crystal exhibits 100% transmittance depicting its excellent transparency over the whole visible region. The electronic transition existing in C=O group of o-chlorobenzoic acid is revealed with the cut-off wavelength of the TCTCDH seen at 238 nm. Hence, these good transparency and cut-off wavelength proposes the grown material to be

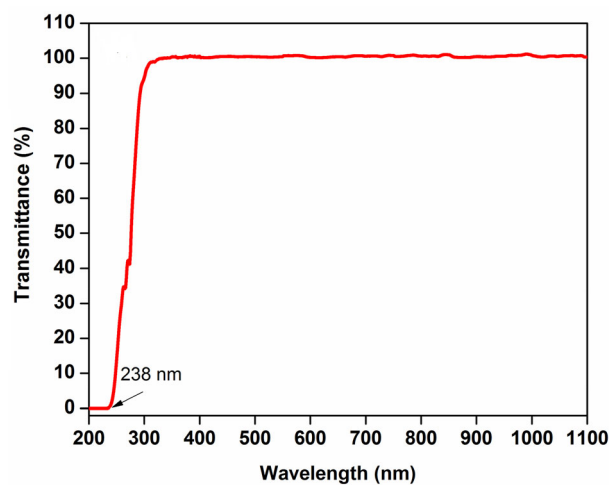
**Table 2** Vibrational frequency assignment of TCTCDH

Absorption (cm <sup>-1</sup> )	Functional group
3444	-NH <sub>3</sub> <sup>+</sup> stretching
2923, 2854	C-H stretching
2146	C-C symmetric stretching
1612	Presence of water molecule
1585	NH <sub>3</sub> <sup>+</sup> symmetrical bending
1369	COO <sup>-</sup> vibrations
1032	C-N symmetric stretching
839	C-Cl stretching
757	COO <sup>-</sup> scissoring
652	COOH rocking
566	C-C=O wagging

compatible with optoelectronic utilizations. The comparison of acquired cut-off wavelength of TCTCDH with so far existing cyclohexylammonium materials is tabulated in Table 5. Using the Tauc's plot [20], the bandgap energy of the TCTCDH crystal was determined and its corresponding graph is shown in Fig. 6. The bandgap energy value of TCTCDH was found to be 5.2 eV.

### 3.4 Dielectric study

The electrical properties such as dielectric constant, dielectric loss, ac conductivity and ac resistivity of TCTCDH single crystal was analyzed using dielectric study. The title crystal was subjected to various range of frequency from 100 Hz to 6 MHz. This analysis was done by employing a well-polished TCTCDH crystal. It was coated with silver paint on both sides

**Fig. 5** UV-visible-NIR transmittance spectrum of TCTCDH

and made it to dry followed by keeping it in between copper electrodes to act as a parallel plate capacitor. The spectrum of dielectric constant of TCTCDH crystal is shown in Fig. 7. From the spectrum, we could observe that the dielectric constant ( $\epsilon$ ) is low at higher frequency whereas it shows higher value at low frequency. This is a general behavior of dielectric material due to the presence of four kinds of polarizations, namely, ionic, electronic, orientation and space charge. At lower frequency, the participation of the above mentioned polarizations will be dynamic. As the frequency decreases, the contribution of these polarizations also decreases [21, 22]. The dielectric constant of TCTCDH single crystal was calculated using the area of the TCTCDH crystal ( $A$ ), thickness of the TCTCDH crystal ( $t$ ) and the capacitance in parallel ( $C_p$ ), this can be expressed using relation (1),

$$\epsilon = c_p t / \epsilon_0 A \tag{1}$$

Another important electrical property is dielectric loss. The dielectric loss of TCTCDH crystal was found by recording for different frequencies and its resultant graph is shown in Fig. 8. From the figure, it was noted that the dielectric loss decreases with increase in the frequency. This shows that grown TCTCDH crystal possesses lesser defects and imperfection [23, 24]. The AC conductivity ( $\sigma_{ac}$ ) of TCTCDH crystal was calculated using the relation (2),

$$\sigma_{ac} = 2\pi f \epsilon \epsilon_0 \tan \delta \tag{2}$$

where  $\tan \delta$  is dielectric loss,  $\epsilon$  is dielectric constant. The AC resistivity of TCTCDH crystal was found by

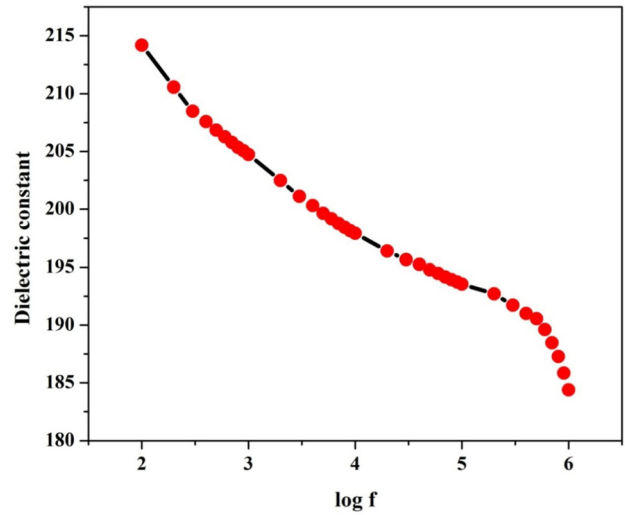


Fig. 7 Dielectric constant vs log f of TCTCDH crystal

taking the reciprocal of ac conductivity. The spectrum of ac conductivity and ac resistivity of TCTCDH crystal are shown in Figs. 9 and 10, respectively.

### 3.5 Nonlinear optical study

Z-scan technique is a powerful tool to analyze intensity dependent third order nonlinear optical properties of materials. This method aids to estimate the nonlinear refractive index ( $n_2$ ), absorption coefficient ( $\beta$ ) and third-order nonlinear optical susceptibility ( $\chi^3$ ) of the samples.

In this technique, CW semiconductor laser beam having wavelength 532 nm uses a convex lens with a

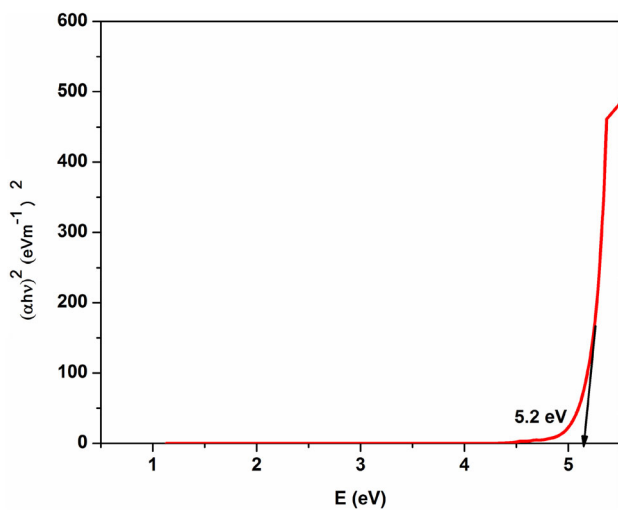


Fig. 6 Tauc's plot of TCTCDH

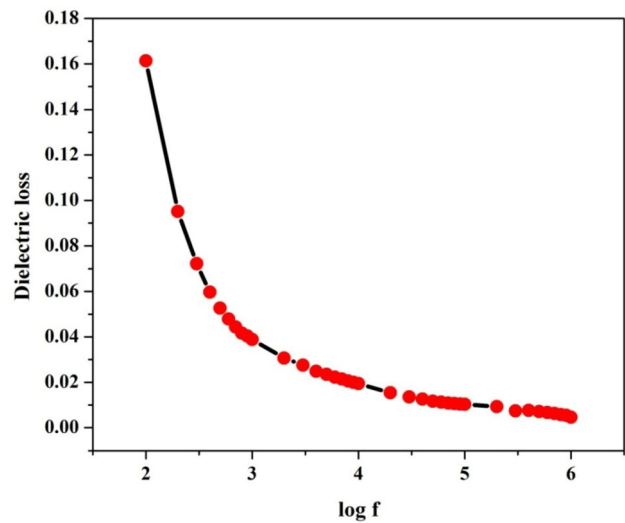


Fig. 8 Dielectric loss vs log f of TCTCDH crystal

focal length of 10.3 cm. Experimental parameters of the Z-Scan technique is presented in Table 3. The sample was rendered through Gaussian laser beam. While moving the sample, the incident intensity falling on the sample varies. The sample to be tested was permitted to translate through positive and negative directions with  $Z = 0$  at the focus of the lens. The related output transmittance of light intensity was noted. The sample was examined in closed and open aperture arrangement where Z-scan traces are gained with and without aperture to calculate nonlinear refractive index ( $n_2$ ) and absorption coefficient ( $\beta$ ) respectively. In addition, all computations were made from the standard equations [25–31].

The nonlinear refractive index ( $n_2$ ) of the TCTCDH single crystal in closed aperture was calculated using the formula given below in Eq. (3).

$$n_2 = \frac{\Delta\Phi}{KI_0L_{eff}} \tag{3}$$

where  $\Delta\Phi$  is the phase shift,  $K$  is wave vector ( $K = 2\pi/\lambda$ ),  $I_0$  is intensity of laser beam at the focus  $Z = 0$  and  $L_{eff}$  is the effective thickness of the TCTCDH crystal.

The absorption coefficient ( $\beta$ ) in open aperture was calculated using the following formula

$$\beta = 2(2\Delta T)^{1/2}/I_0L_{eff} \tag{4}$$

where ‘ $\Delta T$ ’ is peak value at open aperture curve.

The real and imaginary part of the third-order nonlinear susceptibility  $\chi^{(3)}$  were calculated by,

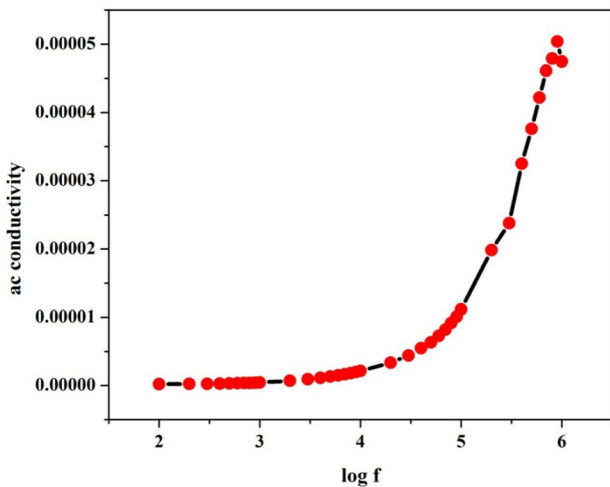


Fig. 9 AC conductivity of TCTCDH crystal

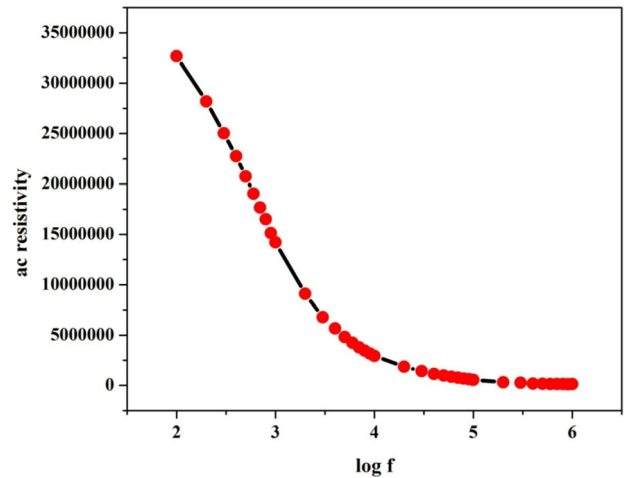


Fig. 10 AC resistivity of TCTCDH crystal

Table 3 Experimental parameters used for Z-scan technique

Laser wavelength and power – 532 nm and 50 mW (Semiconductor – continuous wave laser)
Optical path length – 675 mm
Beam radius at the aperture – 3.5 mm
Radius of aperture – 1.5 mm
Beam radius falling on the lens – 3 mm
Sample thickness – 1 mm
Rayleigh length – 2.16 mm
Laser power $I_0$ – 3.47 kW/cm <sup>2</sup>
Focal length of lens – 103 mm

$$R_e(\chi^{(3)}) \text{ esu} = \frac{10^{-4}\epsilon_0c^2n_0^2n_2}{\pi} \text{ cm}^2\text{w}^{-1} \tag{5}$$

$$I_m(\chi^{(3)}) \text{ esu} = \frac{10^{-2}\epsilon_0c^2n_0^2\lambda\beta}{4\pi^2} \text{ cm}^2\text{w}^{-1} \tag{6}$$

Here  $\epsilon_0$  is vacuum permittivity,  $c$  is the velocity of light and  $n_0$  is the linear refractive index of the crystal.

The  $\chi^{(3)}$  was calculated from the following relation

$$\chi^{(3)} = \left[ \left( R_e \chi^{(3)} \right)^2 + \left( I_m \chi^{(3)} \right)^2 \right]^{1/2} \tag{7}$$

In closed aperture z-scan experiment, the peak followed by valley behavior is the feature of a material with a negative nonlinear refractive index. Figure 11a shows the closed aperture spectrum of TCTCDH crystal. It is found that the peak-valley configuration evaluated from closed aperture scan denotes negative nonlinearity ( $n_2$ ) of TCTCDH material. This infers the

self-defocussing effect which occurs due to the larger beam divergence and reduced transmittance.

In open aperture z-scan experiment, the method in which the calculated transmittance forms a valley at the focus is known as reverse saturable absorption and peak at the focus is known as saturable absorption. The saturable absorption and reverse saturable absorption are well known as negative and positive type of absorption nonlinearity, respectively. The recorded open aperture spectrum of TCTCDH single crystal is shown in Fig. 11b. The absorption coefficient ( $\beta$ ) which has positive sign estimated from open aperture scan confirms reverse saturable absorption of the title compound [25, 32].

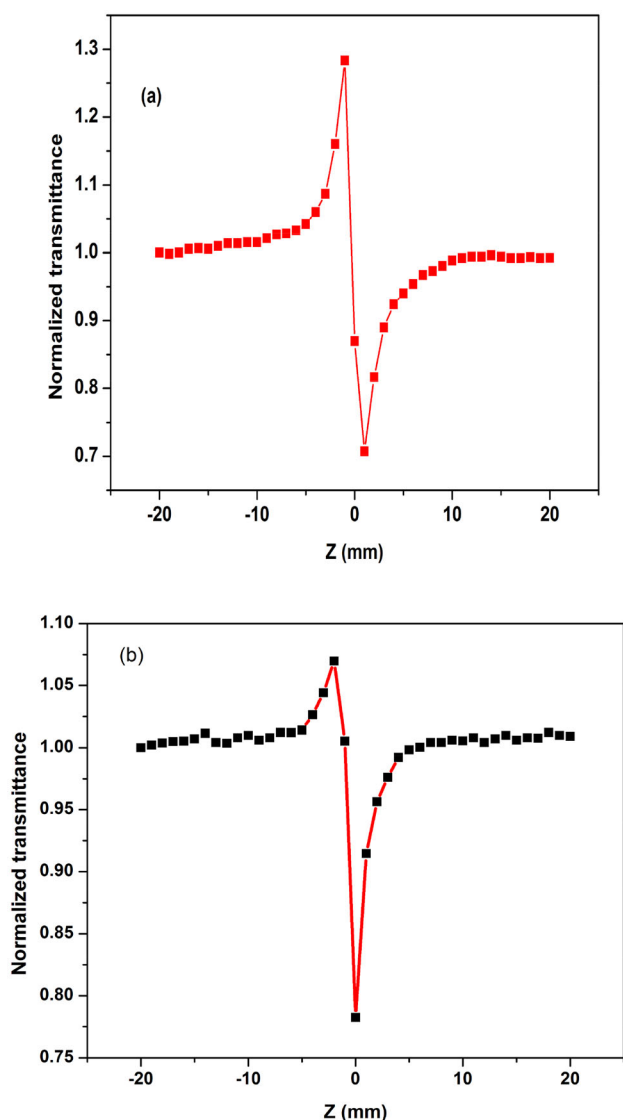


**Fig. 11** (a) Closed aperture curve of TCTCDH crystal (b) open aperture curve of TCTCDH crystal

Experimental estimation of nonlinear refractive index, nonlinear absorption coefficient and optical susceptibility of other cyclohexylammonium based compounds are tabulated in Table 4. It is noted from the observation that the grown material can exhibit NLO properties and it can be utilized for nonlinear optical applications.

### 3.6 Thermal analysis

The TCTCDH crystal was subjected to thermal analysis to disclose their thermal properties by TGA/DSC analysis. The TCTCDH material of 4.350 mg was heated with STA 409 PL thermal analyzer over the range 25–400 °C in nitrogen atmosphere. The TGA/DSC thermogram is shown in Fig. 12. The TG spectrum reveals that the loss of weight has occurred in three steps. The elimination of two water molecules present in the TCTCDH is in agreement with the loss of weight at 125 °C with a mass change of 4.49%. The water molecule consists mass of 32.08 g/mol (experiment 4.49%, calculated 4.48%). This loss of weight is connected with a sharp endothermic peak in DSC trace at 120 °C. Further, the endothermic peak observed at 60 °C in DSC is assigned to the melting point of the compound and it indicates that the TCTCDH material is stable up to 60 °C. The second disintegration has occurred among 125 °C and 265 °C with a loss of weight of about 38.49% (calculated: 39.41%). This is due to the liberation of bis(cyclohexylammonium) bis(o-chlorobenzoate). This weight loss connected with a sharp endothermic peak in DSC trace at 222 °C is recognized to the endothermic energy to break the bonds during the breakdown of the compound. Further, in the temperature range between 265 °C and 300 °C, the compound suffers weight loss as indicated in TGA. It might have associated to the loss of volatile substances such as CO<sub>2</sub>, NH<sub>3</sub> and CO in the compound one by one.

**Table 4** Comparison of nonlinear optical parameters with some of the reported Cyclohexylammonium materials

Compound	$n_2$ (cm <sup>2</sup> /W)	$\beta \times 10^{-4}$ (cm/W)	$\chi^{(3)}$ (esu)
CYHAC [12]	$-4.920 \times 10^{-8}$	0.080	$2.394 \times 10^{-6}$
CYHAD [13]	$-5.124 \times 10^{-8}$	0.024	$2.443 \times 10^{-6}$
BCSSA [15]	$-4.718 \times 10^{-8}$	0.061	$2.274 \times 10^{-6}$
Present work	$-7.26 \times 10^{-9}$	3.88	$7.06 \times 10^{-6}$

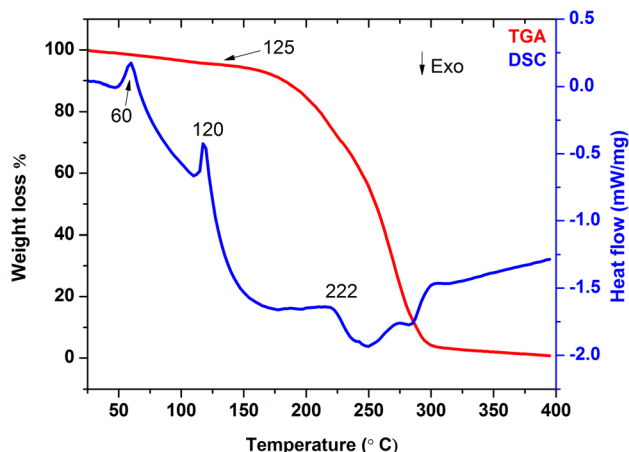


**Fig. 12** TGA-DSC curve of TCTCDH

Sharpness of the endothermic peaks shows the good degree of crystallization of TCTCDH sample. The DSC curve reveals associated changes as shown in TGA curve. From these studies, it is concluded that this TCTCDH material could be exploited for any applications under 60 °C which is comparable with other NLO materials and is given in Table 5.

### 3.7 Vicker's hardness study

The hardness characterization of the substances plays a key factor in the device manufacturing process [33, 34]. A well-polished surface of TCTCDH single crystal was examined for various loads from 25 to 200 g. The Vicker's hardness number of the grown crystal was calculated using the expression (8),

$$H_v = 1.855 (P/d^2) \quad (8)$$

in which,  $H_v$  is the Vickers hardness number in  $\text{kg mm}^{-2}$ ,  $d$  is the diagonal length of the indented impression in mm and  $P$  is the indenter load in kg. The graph was plotted between the variation in hardness number and the applied load and is shown

**Table 5** Comparison of optical and thermal properties of TCTCDH with other cyclohexylammonium materials

Name of the compound	Cut-off wavelength (nm)	Thermal strength (°C)
CYHAC [12]	254	161
CYHAD [13]	252	168
CYHPH [14]	307	146
BHADO [16]	320	75
TCTCDH (present work)	238	60

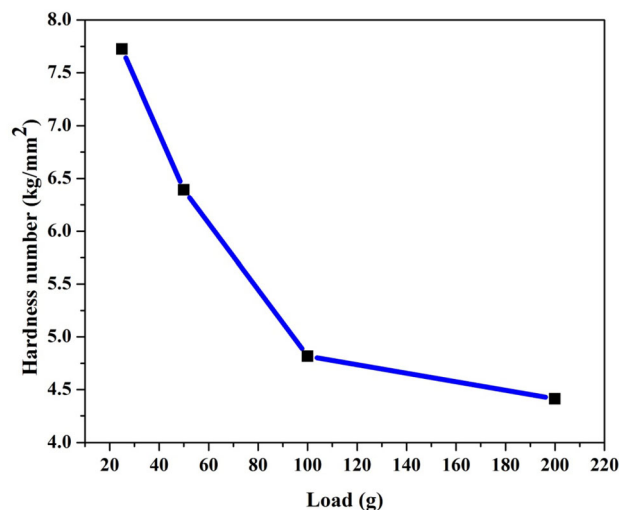


**Fig. 13** Hardness number vs load of TCTCDH single crystal

in Fig. 13. The graph shows that the hardness value decreases as the load increases which is inferred as indentation size effect (ISE). The indentation size and load is related by Meyer's law as follows

$$P = K_1 d^n \quad (9)$$

or

$$\text{Log } P = \text{log } K_1 + n \text{ log } d$$

In which  $K_1$  and ' $n$ ' represent the material constant and work hardening coefficient (Mayer's index) respectively. The value of ' $n$ ' can be evaluated through the value of slope obtained from the graph. Figure 14 shows the plot of  $\text{log } P$  against  $\text{log } d$  and the slope value ' $n$ ' of TCTCDH crystal was to be 0.146 by Mayer's law. Onitsch has stated that the value of ' $n$ ' should lie between 1 and 1.6 for harder materials and above 1.6 for softer materials [35]. When  $n < 2$ , it is the regular ISE behavior and RISE behavior if  $n > 2$  [34, 36]. From this, we could reveal that the grown TCTCDH crystal exhibits indentation size behavior.



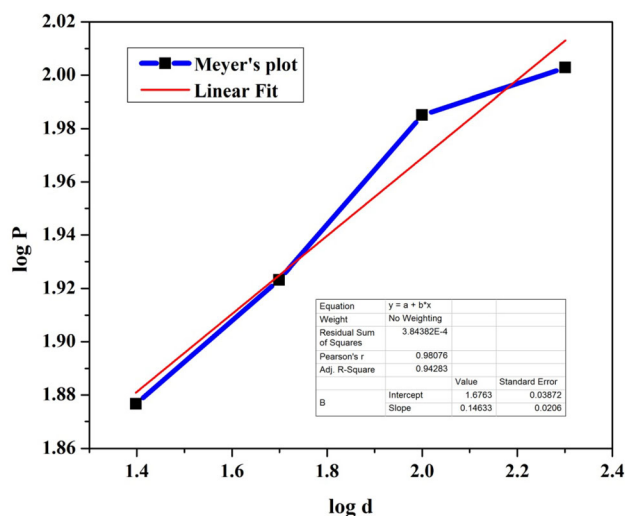


Fig. 14 Meyer's plot of TCTCDH crystal

## 4 Conclusion

Optically good quality nonlinear optical crystals of tris(cyclohexylammonium) tris(o-chlorobenzoate) dihydrate (TCTCDH) had been grown adopting slow evaporation method. The unit cell parameters were confirmed using powder XRD study. Fourier transform IR spectral analysis confirms the functional groups present in the titular compound. The lower cut-off wavelength (238 nm) and the energy bandgap (5.2 eV) were calculated using UV-visible-NIR spectral analysis. The low dielectric constant and low dielectric loss values were observed at higher applied frequencies. From the Z-scan technique, a negative nonlinear refractive index value was observed. The third-order nonlinear susceptibility value of TCTCDH crystal was determined as  $7.06 \times 10^{-6}$  esu. The thermal analyses reveal that the grown crystal is stable upto 60 °C. The Vicker's hardness study showed that the TCTCDH crystal exhibits indentation size effect and it belongs to hard material category. The above results show that the grown TCTCDH crystal could be a potential candidate for the nonlinear optical applications.

## References

1. K. Mohanraj, D. Balasubramanian, N. Jhansi, *Opt. Laser Technol.* **96**, 318–322 (2017)
2. V. Siva Shankar, R. Siddheswaran, R. Sankar, R. Jayavel, P. Murugakoothan, *Curr. Appl. Phys.* **9**, 1125–1128 (2009)

3. D.S. Chemla, J. Zyss, *Nonlinear Optical Properties of Organic Molecules and Crystals* (Academic Press, New York, 1987)
4. P. Prabu, B. Vijayabhaskaran, G. Vasuki, C. Ramachandra Raja, *Opt. Laser Technol.* **98**, 12–18 (2018)
5. S. Debrusa, J. Venturini, N. Pincon, J. Baran, J. Barycki, T. Glowiak, A. Pietraszko, *Synth. Met.* **127**, 99 (2002)
6. M. Loganayaki, P. Murugakoothan, *J. Optoelectron. Adv. Mater.* **5**, 581–586 (2011)
7. R. Anbarasan, P. Eniya, J.K. Sundar, *J. Electron. Mater.* **48**, 7686–7695 (2019)
8. X. Gao, Z. Lin, S. Jin, G. Chen, T. Huang, Z. Ji, Y. Zhou, D. Wang, *J. Chem. Crystallogr.* **44**, 210–219 (2014)
9. C.J. Janiak, *J. Chem. Soc. Dalton Trans.*, 3885–3896 (2000)
10. G.R. Desiraju, *Chem. Commun.* **24**, 2995 (2005)
11. K. Elangovan, M. Boobalan, A. Senthil, G. Vinitha, *J. Mol. Struct.* **1196**, 720–733 (2019)
12. R. Gomathi, S. Madeswaran, D. Rajan Babu, G. Aravindan, *Mater. Lett.* **209**, 240–243 (2017)
13. R. Gomathi, S. Madeswaran, *Mater. Chem. Phys.* **218**, 189–195 (2018)
14. R. Gomathi, S. Madeswaran, D. Rajan Babu, *J. Mater. Sci. Mater. Electron.* **28**, 11374 (2017)
15. R. Gomathi, S. Madeswaran, D. Rajan Babu, *Mater. Chem. Phys.* **207**, 84–90 (2018)
16. K. Senthil, A. Senthil, K. Elangovan, *J. Mol. Struct.* **1209**, 127926 (2020)
17. S. Janarthanan, T.K. Kumar, S. Pandi, D.P. Anand, *Indian J. Pure Appl. Phys.* **47**, 332–336 (2009)
18. M. Suresh, S. Asath Bahadur, S. Athimoolam, *J. Mol. Struct.* **1112**, 71–80 (2016)
19. P. Sathya, M. Anantharaja, N. Elavarasu, R. Gopalakrishnan, *Bull. Mater. Sci.* **38**, 1291–1299 (2015)
20. J. Tauc, R. Grigorovici, A. Vancu, *Phys. Status Solidi B* **15**, 627 (1966)
21. D. Xue, K. Kitamura, *Solid State Commun.* **122**, 537–541 (2002)
22. M. Meena, C.K. Mahadevan, *Cryst. Res. Technol.* **43**, 166–172 (2008)
23. C. Balarew, R. Duhlew, *J. Solid-State Chem.* **55**, 1–6 (1984)
24. S. Suresh, A. Ramanand, D. Jayaraman, P. Mani, *Optoelectron. Adv. Mater.* **4**, 1763–1765 (2010)
25. S. VEDIYAPPAN, R. Arumugam, K. Pichan, R. Kasthuri, S.P. Muthu, R. Perumal, *Appl. Phys. A Mater. Sci. Process.* **29**, 780 (2017)
26. M. Divya Bharathi, G. Ahila, J. Mohana, G. Chakkaravarthi, G. Anbalagan, *J. Phys. Chem. Solids* **98**, 290–297 (2016)
27. RO.MU. Jauhar, V. Viswanathan, P. Vivek, G. Vinitha, V. Devadasan, P. Murugakoothan, *RSC Adv.* **6**, 57977–57985 (2016)

28. K. Senthil, S. Kalainathan, F. Hamada, M. Yamada, P.G. Aravindan, *Opt. Mater.* **46**, 565–577 (2015)
29. P. Asokan, S. Kalainathan, *J. Phys. Chem. C* **121**, 22384–22395 (2017)
30. T.C. Sabari Girisun, S. Dhanuskodi, *Cryst. Res. Technol.* **44**, 1297–1302 (2009)
31. A.N. Vigneshwaran, P. Paramasivam, C.R. Raja, *Mater. Lett.* **178**, 100–103 (2016)
32. M. Sheik-Bahae, A.A. Said, T.H. Wei, D.J. Hagan, E.W. Van Stryland, *IEEE J. Quantum Electron.* **26**, 760–769 (1990)
33. J.H. West Brook, H. Conrad, *The Science of Hardness Testing and its Research Applications* (American Society for Metals, 1973)
34. B.W. Mott, *Micro Indentation Hardness Testing* (Butterworths, London, 1966)
35. E.M. Onitsch, *Mikroskopia* **2**, 131–151 (1947)
36. J. Gong, *J. Mater. Sci. Lett.* **19**, 515 (2000)

**Publisher's Note** Springer Nature remains neutral with regard to jurisdictional claims in published maps and institutional affiliations.